ORIGINAL PAPER

Wear and Friction-Induced Vibration of Brake Friction Materials with Different Weight Average Molar Mass Phenolic Resins

M. W. Shin · J. W. Kim · B. S. Joo · H. Jang

Abstract The friction and wear of brake friction materials containing phenolic resins with different weight average molecular masses (M_w = 2.2–6.1 kg/mol) were investigated using a Krauss-type tribometer and a reduced-scale dynamometer. The results demonstrated that the friction level, wear rate, and friction instability were strongly affected by the M_w of the phenolic resin, attributed to the different shear strengths of the friction materials. The high-M_w phenolic resin exhibited an increased friction level while reducing the wear rate, with both effects more pronounced at temperatures above the phenolic resin decomposition temperature. The friction materials containing the higher-M_w phenolic resins also showed an improved friction instability, revealing a lower critical velocity for the incidence of friction oscillation. The stiffness measured from the friction material revealed that the M_w did not change the surface stiffness after the friction tests, indicating that the improved friction-induced vibration of the friction material with the high-M_w phenolic resin was attributed to an increased matrix stiffness rather than to the sliding surface.

Keywords Brake/clutch materials · Stick-slip · Sliding wear · Phenolic resin · Average molecular mass · Fade · Wear

1 Introduction

The friction material used in automotive brake systems requires durability and long-term friction stability at various braking conditions without excessive wear and noise generation. In order to meet these requirements, brake friction materials have been developed as multiphase composites composed of reinforcing fibers, binder resins, abrasives, solid lubricants, space fillers, and other friction modifiers [1]. Among various constituents used in commercial brake friction materials, binder resins are known to affect various aspects of brake performance [2]. Phenolic resin, which is produced by a chemical reaction between phenol and formaldehyde under alkaline or acidic conditions, has been used since the early development stage of modern friction materials owing to its high-temperature strength and wear resistance after curing [3]. However, phenolic resin has been known to have a strong influence on fade, wear resistance, and noise occurrence; various modifications of the straight phenolic resin have been performed to improve brake performance-related issues such as high wear rate, noise, and high temperature fade [2, 4].

Brake fade is the decrease in friction force at elevated temperatures, and it is closely related to thermal decomposition of the binder resin and degradation of other organic ingredients in the brake friction material [3, 5, 6]. This fade normally accompanies excessive friction material wear, being known as an important cause of the short life span of the friction material. In order to improve the friction effectiveness, which indicates the robustness of the friction level with the change in sliding conditions, and wear resistance of the brake friction materials at elevated temperatures, considerable effort has been conducted on modifying the straight phenolic resin. Kim and Jang [6] showed that the friction level and wear resistance changed according to the type and relative amount of resin that was reinforced with aramid pulp. They found that the resin modified with aralkyl ether stabilized the friction coefficient at elevated temperatures, while the amount of specific

M. W. Shin · J. W. Kim · B. S. Joo · H. Jang (✉)
Department of Materials Science and Engineering, Korea University, 1, 5-ga, Anam-dong, Sungbuk-gu, Seoul 136-713, South Korea
e-mail: hojang@korea.ac.kr

wear increased. Hong et al. [7] studied the wear mechanism as a function of temperature by comparing three different phenolic resins (straight, Si-modified, and B–P-modified). They revealed that the B–P-modified resin had the greatest resistance to high temperature wear due to the high activation energy required for its thermal decomposition. Nidhi et al. [8–10] studied the fade and recovery characteristics of friction materials with various modified resins. They reported that the mechanical and thermal properties of the friction material showed no strong correlation with friction and wear at elevated temperatures. Other studies examining the friction characteristics of various binder resins also showed multifaceted tribological properties from modified resins with improved high-temperature properties [11, 12].

While studies of binder resins concerning the fade and wear resistance of brake friction materials are available in the literature, the effect of the binder resin on the friction-induced noise and vibration is very limited. Nishiwaki et al. [13] demonstrated a new friction material having a reduced friction-induced vibration and noise using a resin with modified molecular chains. They suggested that the higher friction effectiveness and low squeal propensity are attributed to the straight chain structure in a polyamide–imide (PAI) resin. Cho et al. [14] examined the effect of the friction material ingredients on the friction-induced noise propensity. They found that the propensity of friction-induced noise was increased when the friction material contained a larger amount of phenolic resin. However, the root cause of interfacial excitation produced at the sliding interface as a result of the binder resin, along with the associated detailed mechanism for producing brake noise were not understood.

In this study, friction materials with phenolic resins of different weight average molecular masses (M_w) were used to investigate their effect on fade resistance, high temperature wear rate, and friction-induced vibration. This study is a sequel to our previous work on the wear mechanism and friction instability of friction materials with different phenolic resins [7, 15], and here, we focus on the effect of M_w on wear and friction-induced vibration.

2 Materials and Methods

The phenolic resins used in this study are commercial products developed for friction materials (Gangnam Chemical Co., Korea). The average molecular weights of the resins are approximately 2.2, 3.8, and 6.1 kg/mol, and all contain the same amount of hexamine. Table 1 shows the general properties of the phenolic resins used in this work. The friction material specimens were produced based on a simple formulation (Table 2) to avoid spurious ingredient effects from a full formulation that contains more than ten

constituents. The amount of phenolic resin in the formulation was set to 16 vol% to be comparable with commercial brake friction materials. The friction material samples were fabricated following the conventional procedure used to produce commercial products: mixing, preforming, hot pressing, and post-curing. The detailed fabrication conditions for the friction material samples used in this study can be found in a previous study [16]. The surface hardness of the friction material was measured using a Rockwell hardness tester (ARK 600K, Akashi, Japan), and its compressibility was measured with a universal testing machine (UTM-3367, Instron, USA).

Friction tests were performed using a Krauss-type tester (MoinSys, Korea) and a one-fifth-scale reduced dynamometer (NeoPlus, Korea). The Krauss-type tester was used to investigate the fade resistance and wear amount at elevated temperatures. The wear rate was calculated by normalizing the amount of wear by the friction energy (friction force × sliding distance) accompanying the friction test. The friction oscillation was examined by the one-fifth-scale dynamometer, focusing on the friction instability as a function of pressure and sliding velocity. A gray cast iron disk, 160 mm in diameter and 8 mm thick, was used as a counter surface. The humidity in the friction test was maintained at 5.1–8.3 g/m^3. The detailed test procedures for the wear and friction oscillation are listed in Tables 3 and 4. A laser confocal microscope (VK-8710, Keyence, Japan) was used to examine the sliding surfaces before and after the tests and to calculate the roughness parameters.

3 Results and Discussion

3.1 Friction Effectiveness and Wear as a Function of Temperature

The surface hardness and compressibility of friction material samples containing the resins with three different M_w (RMW-L: 2.2 kg/mol, RMW-M: 3.8 kg/mol, and RMW-H: 6.1 kg/mol) were examined before investigating the tribological properties. Figure 1a shows the hardness values of the friction material samples, indicating that the surface hardness increases with the weight average molecular mass of the resin. The compressibility of the friction material, shown in Fig. 1b, decreased when binder resins with higher M_w were used. The high surface hardness (or low compressibility) of the high-M_w resin indicates that it converts to a harder matrix after curing because of the larger average molecular size, which can affect the brake system stiffness and pedal feel during brake application.

The coefficient of friction (COF) was measured as a function of temperature to examine the effect of the M_w on the high-temperature friction effectiveness. Figure 2 shows

Table 1 Hexamine content and general properties of the three different phenolic resins

	RMW-L	RMW-M	RMW-H
Hexamine level: ISO 8988 (%)	7.0	7.0	7.0
Flow distance: ISO 8019 (mm)	47	39	31
Melting point (°C)	76	80	86
Weight average molecular mass (M_W, kg/mol)	2.2	3.8	6.1
Polydispersity (M_W/M_N)	4.1	4.3	4.2

Table 2 Friction material composition investigated in this study

Classification	Ingredient	Vol%
Binder	Phenolic resin	16
Reinforcing fiber	Aramid fiber	15
Filler	Barite	55
Solid lubricant	Graphite	9
Abrasive	Zircon	5

Table 3 Conditions for the Krauss-type tribometer test procedure performed to examine the fade and wear rate

Krauss-type tribometer	Test conditions
Burnish	Velocity = 3 m/s, pressure = 0.7 MPa
	Drag time: 300 s (three times)
Fade and wear test	Fade test: velocity = 3 m/s, pressure = 1 MPa
	Wear test: temperature: 60, 120, 170, 220, 270, 320, 370, 420, and 450 °C
	Pressure = 1 MPa, drag distance: 5 km (each temperature condition)

Table 4 Dynamometer test procedure performed to examine the friction instability at low-speed sliding velocities

One-fifth-scale dynamometer	Test conditions
Burnish	Speed = 70 km/h, pressure = 3 MPa
	Initial brake temperature = 120 °C
	Repeated 200 times in a constant pressure mode
Low-speed drag	Drag velocity = 0.12–15.0 mm/s
	Pressure = 1, 2, 4, and 6 MPa
	Initial brake temperature = 20–25 °C, Humidity = 5.1–8.3 g/m^3 A.H.

Fig. 1 **a** Surface hardness and **b** compressibility of friction materials containing resins with different M_w (RMW-L: 2.2 kg/mol, RMW-M: 3.8 kg/mol, and RMW-H: 6.1 kg/mol)
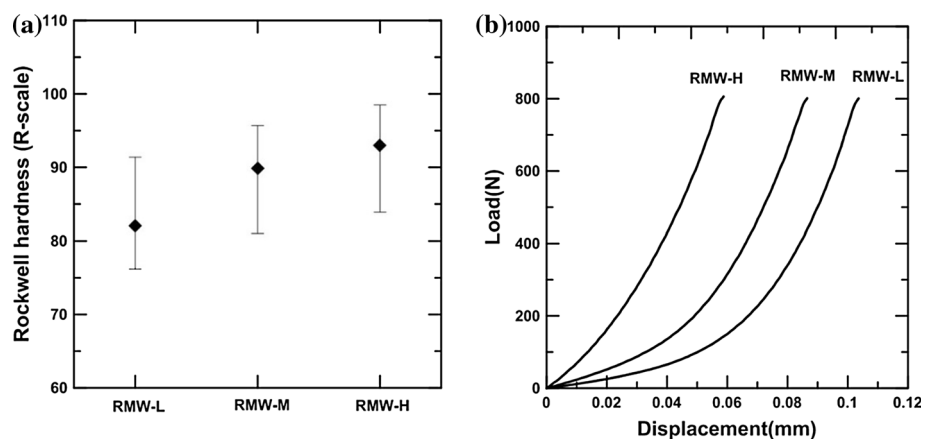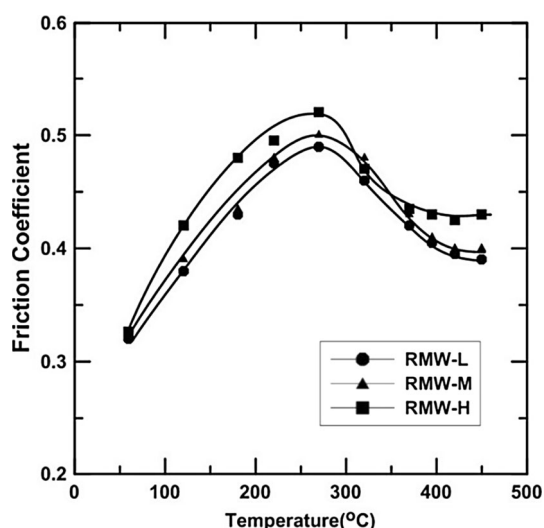
Fig. 2 Friction coefficient measured as a function of disk temperature using a Krauss-type tribometer, for RMW-L (*circles*), RMW-M (*triangles*), and RMW-H (*squares*)

the COF as a function of disk temperature when the sliding test continues up to 450 °C. The increase in the COF below the peak friction temperature is attributed to the increased contact area and the decrease at higher temperature is owing to the thermal decomposition of the binder resins. This is analogous to the results by Hong et al. [7], who also reported the COF as a function of temperature. They showed that the maximum COF temperature increased when the resins were modified by silicon or boron-phosphorus. On the other hand, the peak friction temperature was similar when the drag test was carried out using the resins with different M_w. The similar peak friction temperatures for a single type of resin with different M_w indicate that the chemical modification is more effective for improving fade resistance than increasing the M_w.

The COF level and fade resistance, on the other hand, increased slightly when the M_w of the resin increased, showing the highest COF with the RMW-H over the entire temperature range. This result appears closely related to its molecular length. When the resin undergoes a transition to a rubbery state at elevated temperatures, the high molecular weight resin also assists in sustaining the friction level due to its high viscosity, since the shear strength of phenolic resins is related to their molecular weight [17]. Similar effects of the M_w on the friction and wear properties have also been reported for other binder resins [18]. The worn surfaces of the friction materials after the friction tests support the improved fade resistance of the friction material with high M_w. Figure 3 shows the worn surface of the friction materials after the drag tests using the Krauss-type tribometer, showing larger contact plateaus produced during the sliding at elevated temperatures in the case of the

RMW-H. On the other hand, the RMW-L surface shows few contact plateaus remaining, because of the detachment of decomposed ingredients from the friction surface. The wear rate measured after the high temperature drag tests at 450 °C also supports the severe ingredient detachment from the friction material surface with the RMW-L resin (Fig. 4), indicating that the high temperature wear resistance was improved with the friction material using the highest M_w phenolic resin.

In order to understand the wear mechanism in more detail, the specific wear rates were plotted as a function of temperature and shown in Fig. 5. The specific wear rate was calculated by normalizing the wear amount by the friction energy involved in the sliding friction. The wear rate increased with increasing disk surface temperature, while the temperature-dependent wear rate showed a rapid wear rate increase above the transition temperature. The transition temperatures obtained from the Arrhenius plots in Fig. 5 were 282, 316, and 372 °C for RMW-L, RMW-M, and RMW-H, respectively. This is an interesting finding since the peak friction temperatures obtained from continuous drag tests were similar regardless of M_w in the friction materials. This appears due to the difference in the accumulated thermal history between the two different test modes and because the wear process is more susceptible to destruction of the molecules while the fade in Fig. 2 is affected by the softening of the resin. This also suggests that the wear mechanism is different below and above the transition temperature. The slopes of the two temperature regions were converted to activation energies of the wear process using the Arrhenius equation and are listed in Table 5. The activation energy levels from 60 to 200 °C were similar regardless of the M_w used, and all were small compared with the activation energy for thermal decomposition of the straight phenolic resin [19]. This suggests that the wear process below the transition temperature was not primarily determined by the thermal decomposition, but instead intensely affected by the wear of other ingredients and the counter disks. In comparison, the activation energies above the transition temperature were similar to the activation energy for thermal decomposition of the phenolic resin, as presented in previous investigations [7, 19].

Another interesting finding was the different activation energy values associated with the wear process relative to the phenolic resin M_w. It appears that the wear mechanism above the transition temperature is mainly affected by the scission of polymer chains and carbonization. Similar results can be found in the literature [6, 7, 15], which also indicated that the high temperature wear of the phenolic resin depended on its thermal decomposition. The high activation energy of the RMW-H supports its low wear rate at 450 °C (shown in Fig. 4), suggesting a potential control
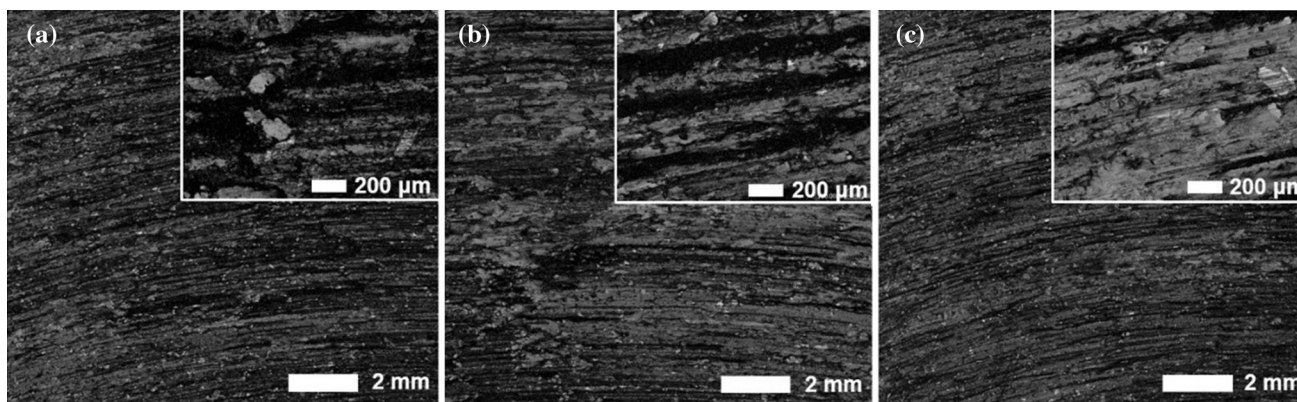
Fig. 3 Worn friction material surfaces containing. **a** RMW-L: 2.2 kg/mol, **b** RMW-M: 3.8 kg/mol and **c** RMW-H: 6.1 kg/mol resins after the friction tests at 450 °C. *Insets* are close-ups of the surface at a higher magnification
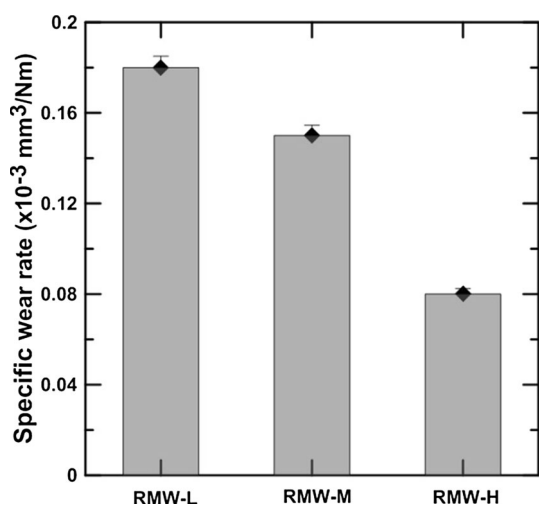

Fig. 4 Wear rate calculated from the friction tests at 450 °C for the friction materials containing RMW-L: 2.2 kg/mol, RMW-M: 3.8 kg/mol and RMW-H: 6.1 kg/mol

of fade and high temperature wear by selecting a proper molecular weight of the phenolic resin.

3.2 Friction Oscillation

The friction-induced vibration during sliding was measured using a 1/5-scale brake dynamometer to investigate the propensity for noise triggered by friction materials with different M_w phenolic resins. It is known that the shape of the friction oscillation changes with sliding velocity, applied pressure, humidity, temperature, and the sliding interface properties such as stiffness and contact area [20–22]. In general, the friction oscillation shows a stick-slip pattern at low sliding speeds, changing to harmonic oscillations at higher speeds, and then finally reducing to a stable friction without periodic oscillation. This is consistent with the interpretation of friction-induced oscillation by Rabinowicz [23] and Gao et al. [24], who suggested that
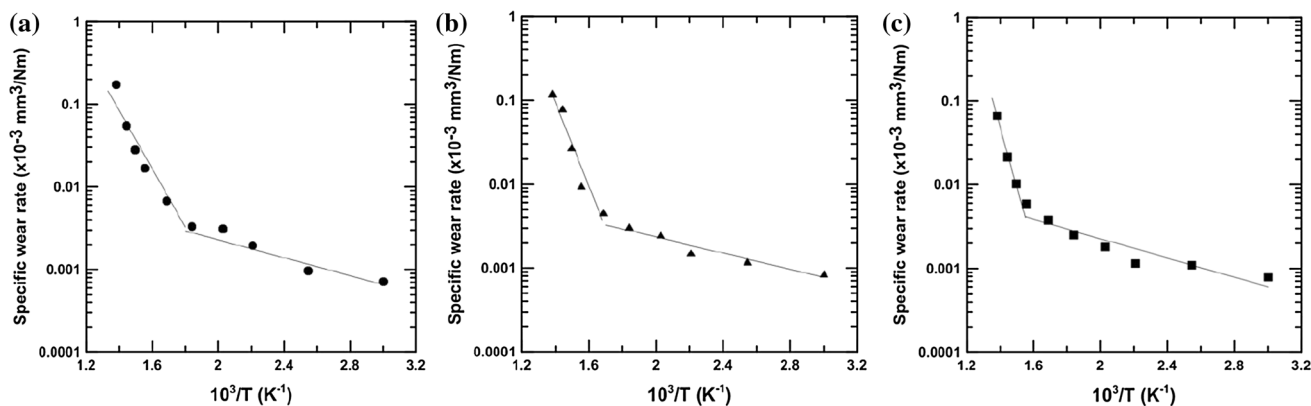

Fig. 5 Wear rates as a function of the inverse absolute temperature (*Arrhenius plots*) obtained from wear tests of friction materials containing, **a** RMW-L: 2.2 kg/mol (*circles*), **b** RMW-M: 3.8 kg/mol (*triangles*), and **c** RMW-H: 6.1 kg/mol (*squares*)

Table 5 Activation energy before and after the transition temperatures obtained from the Arrhenius plots in Fig. 5

Resin type	Activation energy (60–220 °C) kcal/mol	Activation energy (300–450 °C) kcal/mol
RMW-L	5.63	14.2
RMW-M	4.15	15.2
RMW-H	7.49	23.5

the amplitude of the stick-slip is proportional to L/kv, where k is the stiffness of the sliding system, v is the velocity, and L is the applied load.

In order to analyze the friction-induced oscillation from friction materials with different phenolic resins, the type of oscillation was plotted as a function of sliding velocity and applied pressure [22, 25, 26]. The plots in Fig. 6 represent the domains for each type of oscillation, including stick-slip, mixed, harmonic, and smooth sliding. The figure indicates that the friction oscillation is observed to a higher critical velocity when the friction material contains the low-M_w resin. The higher propensity of friction oscillation from the friction material with the low-M_w resin appears to be attributed to its low stiffness.

To investigate the correlation between friction oscillation and contact stiffness of the friction material specimens, the contact stiffness was measured using a 10-mm-diameter steel ball using a universal tester in a compression test mode. By using the steel ball, the contact stiffness of the friction material can be analyzed based on two stiffness values in series, namely the surface stiffness (k_s) and the matrix stiffness (k_m). This is because the ratio of the two stiffness (k_s/k_m) affects the friction instability during sliding [27–29]. Figure 7a shows the pressure–displacement curve obtained from the burnished friction material

surfaces. This figure indicates that the M_w of the resin significantly affected the later stage of indentation at high pressure, implying a higher matrix stiffness of the RMW-H friction material over the others. This is because the slope of the pressure–displacement curve represents the instantaneous normal contact stiffness (k_n). Figure 7b shows the normal stiffness as a function of pressure, which comprises the surface stiffness (k_s) and the matrix stiffness k_m, following: $k_n = (k_s \cdot k_m)/(k_s + k_m)$ [27]. The stiffness profiles in Fig. 7 indicate that the surface stiffness was similar regardless of the resin type, but the matrix stiffness was significantly affected by the type of resin.

The height distribution of the friction material surface was examined after friction tests since the surface morphology has affected the friction and wear of the brake friction materials [25]. In particular, the smooth friction surface with narrow height distribution has shown higher friction levels with pronounced stick-slip and is known to be susceptible to humidity of the environment. The surface roughness effect on these friction characteristics is closely related to the real contact area and its influence on the static coefficient of friction. However, the surface height distribution of the friction material surface after tests was similar as shown in Fig. 8, suggesting that the surface properties did not play a significant role in determining the friction oscillation regardless of the resin M_w. This is also supported by the similar surface stiffness in Fig. 7.

The narrow velocity range for friction oscillation from the friction material with the high-M_w resin in Fig. 6 is, therefore, attributed to its high matrix stiffness, which is consistent with the results from a study by Nakano and Fuadi [28, 29]. They reported that a friction material with a high matrix stiffness and low surface stiffness exhibited smooth sliding, which is analogous to our results. Therefore, the low propensity for friction instability observed in
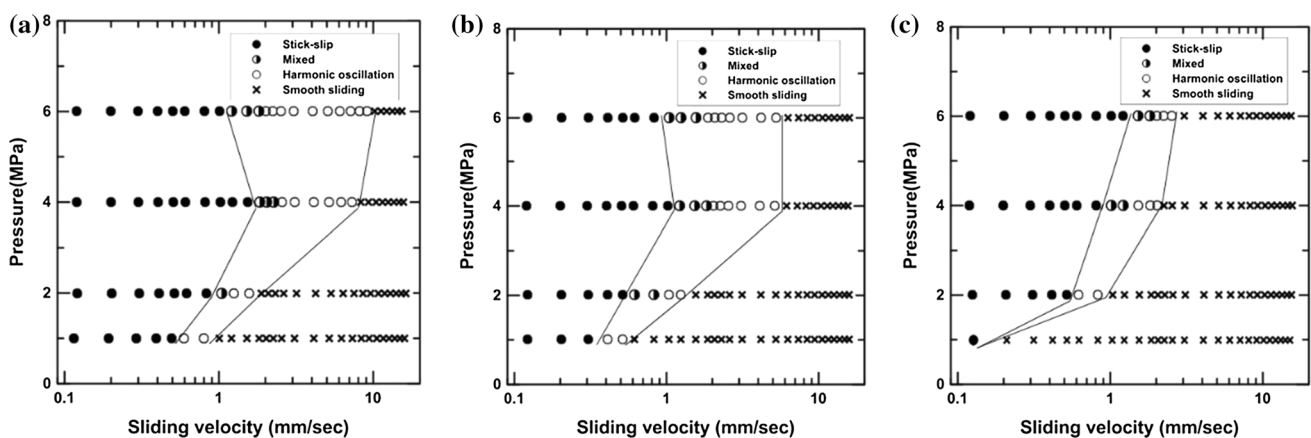
Fig. 6 Friction stability map indicating the type of friction oscillation as a function of pressure and velocity. The maps show domains corresponding to stick-slip (*solid circles*), mixed (*half circles*), harmonic oscillation (*open circles*), and smooth sliding (*cross hatches*) when friction tests were performed on friction materials with **a** RMW-L: 2.2 kg/mol, **b** RMW-M: 3.8 kg/mol, and **c** RMW-H: 6.1 kg/mol

Fig. 7 **a** Pressure–displacement plot and **b** normal contact stiffness (k_n) as a function of pressure, converted from the curves in (**a**). The *dash* and *dash-dot lines* indicate the stiffness of the matrix and surface, respectively, changed as a function pressure
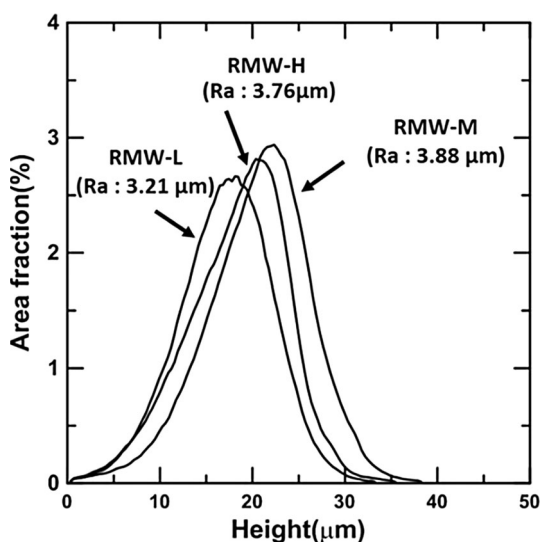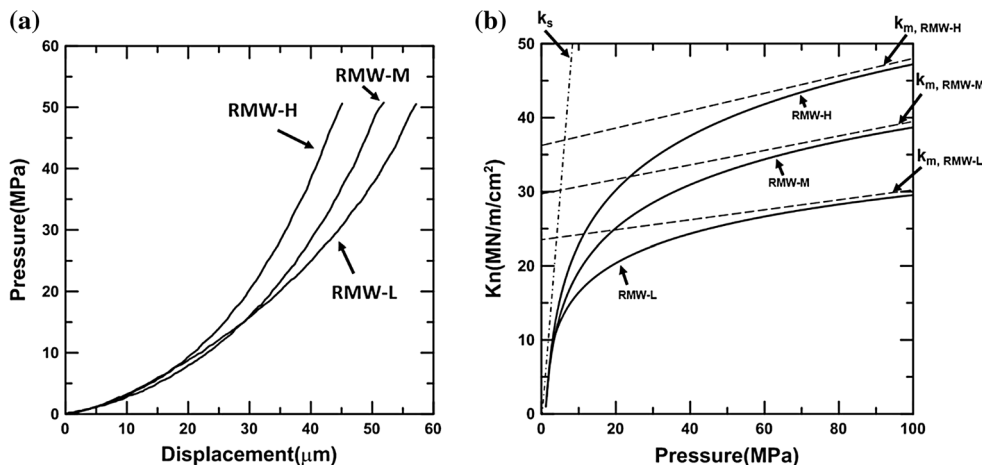

Fig. 8 Height distribution of surface asperities with surface roughness average (R_a) measured from the burnished surface of the friction materials with different resins

Fig. 9 A schematic illustrating the stick-slip amplitudes produced by the friction materials with different matrix stiffness

the friction material with the high-M_w resin is attributed to the matrix stiffness being enhanced by the polymer chains of the phenolic resin rather than by the sliding surface stiffness in our case, which is supported by the stick-slip generation mechanism suggested by Rabinowicz [23] and Gao et al. [24].

The stick-slip phenomenon shown in Fig. 6 is illustrated using a schematic diagram in Fig. 9. It shows the increase in the static coefficient of friction (μ_s) and the dynamic friction coefficient (μ_k) as a function of the sliding time in a stick mode [30]. The static friction coefficient increased rapidly in the early stage, becoming saturated with the stick time, whereas the kinetic friction coefficient (μ_k) increased linearly. When the two coefficients are equal, the stick changes to slip and produces a friction oscillation with the amplitude in the size of the difference between the two coefficients. The schematic also shows that the friction oscillation ceases
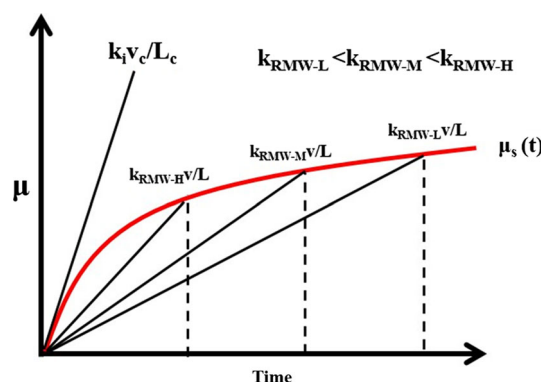
when the slope of μ_k exceeds the critical condition ($k_i v_c/L_c$). The similar roughness values of the friction material surfaces in this case indicate similar $\mu_s(t)$ profiles regardless of resin type, and the stick-slip amplitude is determined by the slope of $\mu_k(t)$. This suggests that stick-slip characteristics is dependent on the stiffness of the friction material since the slope of $\mu_k(t)$ is inversely proportional to matrix stiffness of the friction material since surface properties are similar regardless of the resin M_w. Therefore, the stick-slip amplitude from RMW-L is greater than that from RMW-H when the applied load and sliding velocity are identical. In the same manner, the friction material with the RMW-L resin shows a higher critical velocity for smooth sliding, indicating a higher propensity for friction instability, and showing that the velocity range exhibiting stick-slip is broader in the case of the RMW-L resin.

4 Conclusions

This study investigated the friction and wear of brake friction materials containing a phenolic resin with three

different weight average molecular masses, M_w (RMW-L: 2.2 kg/mol, RMW-M: 3.8 kg/mol, and RMW-H: 6.1 kg/mol). The results showed that the friction instability during sliding, in addition to the friction effectiveness and wear at high temperatures, was strongly affected by the molecular weight of phenolic resin. The friction material with the higher-M_w phenolic resin exhibited a high friction level and low wear rate. This trend was more pronounced at temperatures above the decomposition temperature when the wear mechanism relied on chain scission and resin carbonization at high temperatures. The friction material containing the higher-M_w resin also showed improved performance in the friction-induced vibration, displaying a narrow range of friction oscillation occurrence, which is affected by a high matrix stiffness with low critical velocity for smooth sliding. This suggests that the weight average molecular mass (M_w) of the binder resin can be an important factor for controlling friction effectiveness, wear rate, and friction instability, as much as the resins modified by various chemical processes.

References

1. Jang, H.: Brake friction materials. In: Wang, Q., Chung, Y.-W. (eds.) Encyclopedia of Tribology, pp. 263–273. Springer, New York (2013)
2. Jang, H.: Brake friction materials. In: Sinha, S.K., Briscoe, B.J. (eds.) Polymer Tribology, pp. 521–549. Imperial College Press, London (2009)
3. Jacko, M.G., Tsang, P.H.S., Rhee, S.K.: Automotive friction materials evolution during the past decade. Wear **100**(1–3), 503–515 (1984)
4. Gardziella, A., Pilato, L.A., Knop, A.: Phenolic Resins: Chemistry, Applications, Standardization, Safety and Ecology. Springer, New York (2000)
5. Bijwe, J.: Composites as friction materials: Recent developments in non-asbestos fiber reinforced friction materials—a review. Polym. Compos. **18**(3), 378–396 (1997)
6. Kim, S.J., Jang, H.: Friction and wear of friction materials containing two different phenolic resins reinforced with aramid pulp. Tribol. Int. **33**(7), 477–484 (2000)
7. Hong, U.S., Jung, S.L., Cho, K.H., Cho, M.H., Kim, S.J., Jang, H.: Wear mechanism of multiphase friction materials with different phenolic resin matrices. Wear **266**(7–8), 739–744 (2009)
8. Nidhi, Bijwe, J.: NBR-modified resin in fade and recovery module in non-asbestos organic (NAO) friction materials. Tribol. Lett. **27**(2), 189–196 (2007)
9. Nidhi, Bijwe, J., Mazumdar, B.J.: Influence of amount and modification of resin on fade and recovery behavior of non-asbestos organic (NAO) friction materials. Tribol. Lett. **23**(3), 215–222 (2006)
10. Bijwe, J., Nidhi, Majumdar, N., Satapathy, B.K.: Influence of modified phenolic resins on the fade and recovery behavior of friction materials. Wear **259**, 1068–1078 (2005)
11. Kim, Y.C., Cho, M.H., Kim, S.J., Jang, H.: The effect of phenolic resin, potassium titanate, and CNSL on the tribological properties of brake friction materials. Wear **264**(3–4), 204–210 (2008)
12. Gurunath, P.V., Bijwe, J.: Friction and wear studies on brake-pad materials based on newly developed resin. Wear **263**(7–12), 1212–1219 (2007)
13. Nishiwaki, M., Abe, K., Yanagihara, H., Stankovic, I., Nagasawa, Y., Wakamatsu, S.: A study on friction materials for brake squeal reduction by nanotechnology. No. 2008-01-2581. SAE Technical Paper (2008)
14. Cho, M.H., Kim, S.J., Kim, D., Jang, H.: Effects of ingredients on tribological characteristics of a brake lining: an experimental case study. Wear **258**(11–12), 1682–1687 (2005)
15. Shin, M.W., Cho, K.H., Lee, W.K., Jang, H.: Tribological characteristics of binder resins for brake friction materials at elevated temperatures. Tribol. Lett. **38**(2), 161–168 (2010)
16. Shin, M.W., Kim, Y.H., Jang, H.: Effect of the abrasive size on the friction effectiveness and instability of brake friction materials: a case study with Zircon. Tribol. Lett. **55**(3), 371–379 (2014)
17. Stachowiak, G.W., Batchelor, A.W.: Wear of non-metallic materials. In: Stachowiak, G.W., Batchelor, A.W. (eds.) Engineering Tribology, 3rd edn, pp. 651–704. Butterworth-Heinemann, Boston (2005)
18. Shin, M.W., Kim, S.S., Jang, H.: Friction and wear of polyamide 66 with different weight average molar mass. Tribol. Lett. **44**(2), 151–158 (2011)
19. Auerbach, I.: Decomposition kinetics of a phenolic-carbon composite. I. Resin available for volatilization. J. Appl. Polym. Sci. **14**, 747–756 (1970)
20. Lee, S.M., Lee, W.G., Kim, Y.H., Jang, H.: Surface roughness and the corrosion resistance of 21Cr ferritic stainless steel. Corros. Sci. **63**, 404–409 (2012)
21. Lee, W.K., Shin, M.W., Kim, S.H., Jang, H., Cho, M.H.: The influence of humidity on the sliding friction of brake friction material. Wear **302**(1–2), 1397–1403 (2013)
22. Kim, S.H., Jang, H.: Friction and vibration of brake friction materials reinforced with chopped glass fibers. Tribol. Lett. **52**(2), 341–349 (2013)
23. Rabinowicz, E.: The intrinsic variables affecting the stick-slip process. Proc. Phys. Soc. **71**(4), 668–675 (1958)
24. Gao, C., Kuhlmann-Wilsdorf, D., Makel, D.D.: The dynamic analysis of stick-slip motion. Wear **173**(1–2), 1–12 (1994)
25. Lee, S.M., Shin, M.W., Jang, H.: Friction-induced intermittent motion affected by surface roughness of brake friction materials. Wear **308**(1–2), 29–34 (2013)
26. Park, C.W., Shin, M.W., Jang, H.: Friction-induced stick-slip intensified by corrosion of gray iron brake disc. Wear **309**(1–2), 89–95 (2014)
27. Kosaka, K., Nishizawa, Y., Kurita, Y., Oura, Y.: Influence of pad surface texture on disc brake squeal. No. 2011-01-2354. SAE Technical Paper (2011)
28. Nakano, K., Maegawa, S.: Stick-slip in sliding systems with tangential contact compliance. Tribol. Int. **42**(11–12), 1771–1780 (2009)
29. Fuadi, Z., Adachi, K., Ikeda, H., Naito, H., Kato, K.: Effect of contact stiffness on creep-groan occurrence on a simple caliper–slider experimental model. Tribol. Lett. **33**(3), 169–178 (2008)
30. Dokos, S.J.: Sliding friction under extreme pressures-1. J. Appl. Mech. **13**(2), A148–A156 (1946)